Fluorimetric oxygen sensor with an efficient optical read-out for *in vitro* cell models

Hannu Välimäki[a]*, Jarmo Verho[a], Joose Kreutzer[a], Dhanesh Kattipparambil Rajan[a], Tomi Ryynänen[a], Mari Pekkanen-Mattila[b], Antti Ahola[a], Kirsi Tappura[c], Pasi Kallio[a], Jukka Lekkala[a]

[a]*BioMediTech Institute and Faculty of Biomedical Sciences and Engineering, Tampere University of Technology, Korkeakoulunkatu 3, FI-33720 Tampere, Finland*
[b]*BioMediTech, Faculty of Medicine and Life Sciences, University of Tampere, FI-33014, Tampere, Finland*
[c]*VTT Technical Research Centre of Finland Ltd, Tekniikankatu 1, FI-33720 Tampere, Finland*

**Corresponding author: hannu.valimaki@tut.fi*

Abstract

This paper presents a phase fluorimetric sensor for the monitoring of the oxygen concentration in *in vitro* cell models. The sensing surface of the sensor consists of oxygen sensitive fluorescent dyes (platinum(II) octaethylporphyrinketone) embedded in a thin polystyrene film. In order to optimize the optical read-out scheme of the sensor, we carried out electromagnetic simulations of a fluorescently doped polystyrene film deposited on a glass-water interface. The simulation results showed highly anisotropic angular emission distribution with the maximum irradiance being at super critical angles, which attracts tailored optical designs to maximize the fluorescence collection efficiency. For this purpose, we applied an efficient optical read-out scheme based on an in-contact parabolic lens. The use of parabolic lens also facilitates confocal total internal reflection excitation from the substrate side. This makes the excitation effective and insensitive to biofouling or other optical changes in the sensing surface and, more importantly, greatly reduces the amount of excitation power radiated into the cell culture chamber. Experimental results show that when applied together with phase fluorimetric lifetime sensing, this optical scheme allows one to use thin films (< 500 nm), dilute dye-polymer ratios (0.025%), low power LED excitation (< 2 mW), and yet achieve over 40 dB signal-to-noise ratio at 10 Hz data rate at physiologically relevant oxygen concentrations. These features are important in cell studies, as the potential cytotoxicity of the dyes and the sensing method (i.e. the production of singlet oxygen) are mitigated by the low dye content and excitation power. In addition, thin and dilute polystyrene films are highly transparent and facilitate optical microscopy. We conclude the study by presenting experimental results where the device is applied together with on-line microscopy to an oxygen tension stress study of beating cardiomyocyte cultures.

Keywords: Fluorimetric oxygen sensor; Thin film fluorescence; Enhanced optical read-out; *in vitro* cell models; PtOEPK; Cardiac cells

1. Introduction

As the cellular oxygen level in mammalian tissues is highly regulated [1], a careful control of the oxygen tension is very important also in *in vitro* cell culturing and disease models. Ideally, when studying any cell model, one should be able to both maintain a stable oxygen tension, similar to the one in the corresponding tissue *in vivo*, and, if desired, generate timely changes in order to study the model responses.

The regulation of oxygen levels requires a reliable monitoring system, and especially in microfluidic cell cultures, this is a challenging task. Leaving out all the laboratory methods based on sampling (such as Winkler titration), or sophisticated, expensive and bulky instruments (such as functional Magnetic Resonance Imaging), one is left to make a choice between Clark-type O_2 –electrodes, and optical methods based on oxygen-dependent quenching of photoluminescence [2]. Clark-type O_2 –electrodes have been applied in microfluidic devices [3], but they consume oxygen and are easily contaminated by cell culture constituents, which can result in unstable sensor characteristics in long-term measurements [4]. On the other hand, optical methods do not consume oxygen, are non- or

minimally invasive, quite easily miniaturized and compatible with imaging set-ups [5], which makes them a very attractive choice. It is therefore no wonder that there has been a great progress in the development of optical oxygen probes, polymer matrix materials, and related measurement devices during recent decades. Today many commercial devices based on the oxygen-dependent quenching exist, and extensive technology reviews are available [2, 4, 5, 6].

A typical sensor layout consists of a luminescent dye embedded in a polymer matrix deposited on a solid substrate such as glass, planar waveguide, well plate or optical fibre [6]. However, with some excellent exceptions [7-9], relatively little attention has been paid to the efficiency of the optical detection in the planar sensing scheme, and typically, the detector is placed directly under the substrate. However, when fluorescent oxygen detection is applied in cell cultures, the optical detection efficiency becomes important. Efficient detection scheme enables one to use lower dye/polymer ratios, thinner sensing films and less excitation power without significantly deteriorating the sensor characteristics. These features can greatly mitigate the potential cytotoxicity of the dyes and the sensing method i.e. the production of singlet oxygen [10].

In this paper, we aim at a design and demonstration of an improved optical detection scheme for luminescent oxygen sensing films. For this purpose, we start by presenting numerical simulations of the emission characteristics of thin, fluorescently doped polystyrene films deposited at a water-glass interface. The starting point for the simulations comes from the work of Lukos et al [11] and, especially, from Frischeisen et al [12] and Nowy et al [13], who, in their work related to the organic LEDs, studied the effect of molecular dipole orientation in doped fluorescent organic thin films. Excellent work has also been carried out by Polerecky et al [9], who theoretically studied the radiation characteristics of dipoles within an arbitrary planar multilayer system. After analysing the radiation pattern of a thin dye-polymer film, we present an efficient fluorescent detection scheme based on the works of Enderlein et al [14], Kurtzbuch et al [15] and Välimäki et al [16], who all applied in-contact detection of super critical angle fluorescence to biosensing. In the experimental section, we first study the sensor characteristics of a phase fluorimetric device equipped with the suggested sensing scheme. Here, among the many possibilities for the oxygen sensitive dye and polymer matrix, we chose the combination of platinum(II) octaethylporphyrinketone (PtOEPK) and polystyrene (PS). Polystyrene was chosen, because it possesses many desired properties for the oxygen sensing surface in cell cultures. It has good optical and mechanical properties, and is a widely used a cell culture dish material. In addition, it is relatively gas permeable, and when mixed with a porphyrin dye like PtOEPK, it is very suitable for oxygen sensing at physiological oxygen ranges [5]. The phase fluorimetric detection principle was chosen, because it offers a relatively uncomplicated and cost-effective instrumentation for a single spot oxygen sensing, when compared to time-domain methods that typically require accurate gating and high-speed detectors, and have their advantage typically in direct imaging set-ups [6]. After studying the performance of the device and used collection optics, we conclude our paper by presenting and discussing the experimental results where the device is applied together with on-line microscopy in a pO_2 tension stress study of beating cardiomyocyte cultures.

2. Efficient optical read-out

Thin film fluorescence

Consider an ideal, polystyrene-PtOEPK film with thickness *d*, deposited on a glass-water interface (Fig. 1). Here we assume that the emitting PtOEPK molecules can be treated as oscillating electric dipoles (λ = 750 nm) that are homogenously distributed throughout the whole film thickness. As in typical state-of-the-art oxygen sensing films, we assume that the PtOEPK molecules are only physically entrapped in the polystyrene matrix [17], and have therefore completely random dipole orientation. To numerically simulate the emission distribution of such a film within the dielectric stack formed by the semi-infinite glass and water layers, we followed the methodology presented in [12-13] and simulated separately the contributions of vertically (p_z) and horizontally (p_x and p_y) oriented electric dipoles placed at a set of definite distances $z \in [0 \ldots d]$ from the polystyrene-glass interface and then summed up the contributions. Fig. 2a shows the simulated results for five

homogenous films with thicknesses between 100 nm and 500 nm. The curves show that the actual distribution depends strongly on the film thickness, but also that in all cases the main part of the emission is towards the glass, and that the peak irradiance is found at or above the direction of the critical angle $\theta_c = sin^{-1}(n_w/n_g) = 61.7°$ between water and glass (marked with dashed line). Note also that only a relatively moderate amount of power is radiated below the critical angle $\theta_c = 41.5°$ between the glass and air (dotted line). This represents the part of the irradiation that maximally can be detected with non-contact optics.

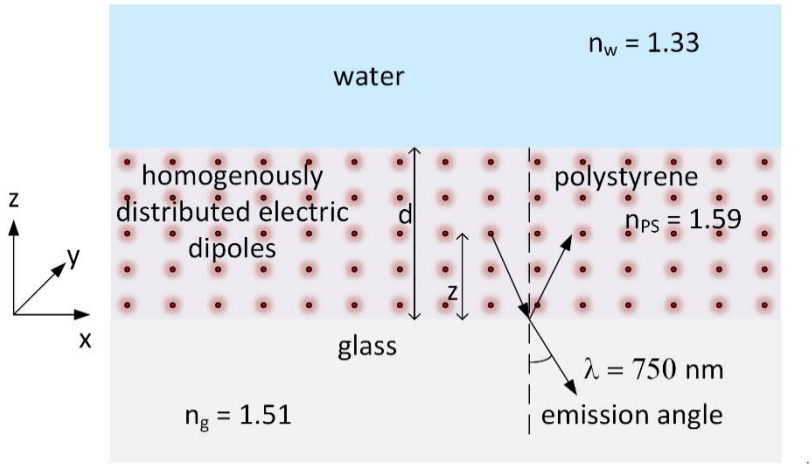

Fig. 1. The modelling scheme of the fluorescent molecules embedded homogenously in a thin polystyrene matrix at a glass-water interface.

Fig. 2b shows, as a function of the film thickness, the simulated relative irradiation (i.e. the power divided by the total radiated power) into the glass space (blue), the contribution of trapped light i.e. the part of the emission that cannot be detected with non-contact optics (red), and the amount that a non-contact lens with the numerical aperture of NA = 0.45, placed underneath the glass plate, could maximally collect (green). It is instructive to realize that with all the simulated film thickness values, only about 1/7 of the radiation emitted into the glass space (or about 1/10 of the total emitted power) can reach the detector when such a typical non-contact sensing scheme is applied.

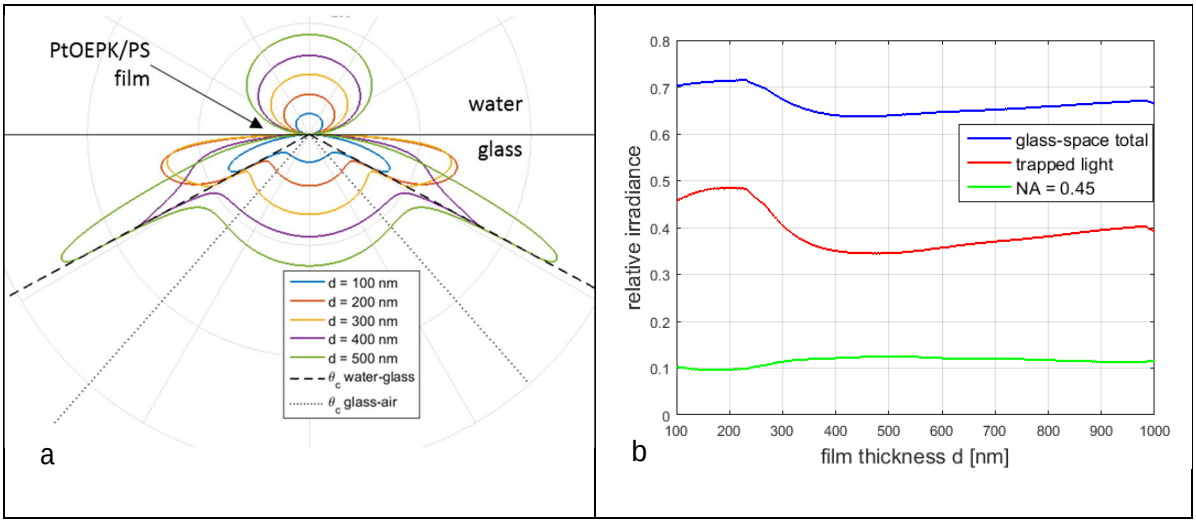

Fig. 2. (a) The angular emission distribution of polystyrene films with varying thickness d, doped with fluorescent dyes emitting at 750 nm; (b) the relative irradiance towards glass-space (blue), the amount of trapped light (red) and the collection efficiency of a lens with NA = 0.45 (green) as a function of film thickness d.

Optical read-out

An efficient way to collect the trapped light is to apply a parabolic lens [14-16] or other kind of refractive and reflective structures [7,8] in optical contact with the substrate, which guide the trapped light to the detector. Here we apply the arrangement shown in Fig. 3a, where the parabolic lens is truncated so that the focal point of the lens is at the glass-water interface, similarly as in a previous set-up targeted to surface sensitive biosensing [16]. The parabolic lens used in the set-up has a focal length of f = 2.78 mm, and the upper and lower diameters of 13.00 mm and 24.90 mm, respectively. With this geometry, the fluorescent emission radiated into the angles between 48.1° and 81.2° can be collected. As Fig. 3b shows, this range fits especially well when the film thickness d = 100, 400 or 500 nm, that is, when the peak irradiance is in the centre of the angular detection range.

If the emission collection efficiency is the parameter to be maximized, then both the direct radiation and trapped light should be collected. A sophisticated way to accomplish this would be to manufacture an integrated lens structure in the centre of the bottom surface of the parabolic lens. With an integrated convex surface, the emission that enters into the paraboloid but is not reflected at the parabolic surface could be collected with greater efficiency. As a first small angle approximation, a convex surface with the radius of curvature of $R = L\,(n_g - 1)/n_g$, where L is the distance between the polystyrene film and the lower surface of the parabolic lens, could be used [18]. We, however, wanted to use the central area of the parabolic lens for microscopy illumination and left this option out.

In the scheme, the parabolic lens is also used for the total internal reflection excitation. The parabolic surface – again through the total internal reflection – focuses the parallel output beam of the excitation LED to the focal point of the parabolic lens. This makes the excitation effective and insensitive to biofouling or other optical changes in the sensing surface. The totally reflected excitation beam is blocked with a plastic blocker below the parabolic lens, which prevents any long wavelength tail of the excitation LED to enter the detector. The total internal reflection excitation arrangement significantly reduces the excitation power radiated into the culture chamber, which diminishes both the direct illumination stress and the possibility of generating singlet oxygen by unintentionally exciting the dyes that could have migrated from the polymer matrix closer to cell membranes. Finally, as both the excitation and the main part of read-out are strictly focused on sensing film, the arrangement is insensitive to autofluorescence and other background signals stemming from the sample side.

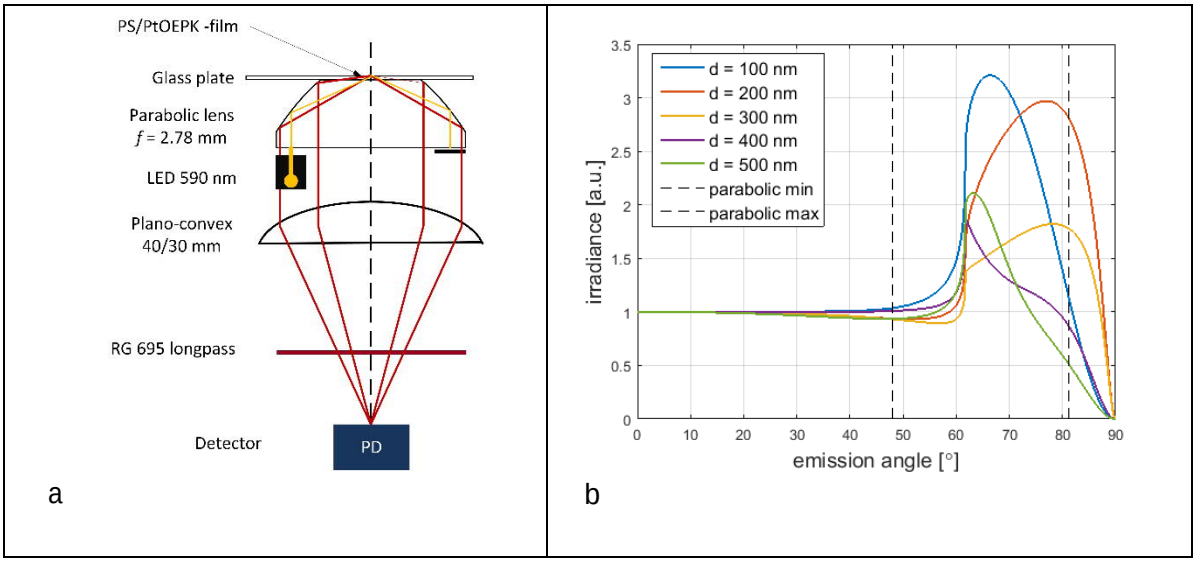

Fig. 3. (a) The optical set-up based on a truncated parabolic lens; (b) The relative emission irradiance (scaled by power emitted directly downwards) vs emission angle with varying film thickness d. The minimum and maximum detectable supercritical angles with the used parabolic lens are marked with dashed lines.

When it comes to the fluorimetric oxygen sensing, fluorescence lifetime based methods – being insensitive to variations in excitation power, dye concentration, photo bleaching, and other gain-type factors – are preferable to direct irradiance-based methods [19]. By modulating the excitation amplitude and measuring the phase between the excitation and emission signals one can make a lifetime-based oxygen sensing scheme that is well described by the Stern-Volmer equation

$$\frac{\phi_0}{\phi} = 1 + K_{sv}\, pO_2 \tag{1}$$

where ϕ_0 and ϕ are the measured phase values in the absence and presence of oxygen, respectively; K_{sv} is Stern-Volmer constant and pO_2 is the oxygen partial pressure.

3. Materials and methods

Oxygen sensing plates
Polystyrene pellets (m_w = 200 000, from Sigma, St. Louis, USA) were dissolved in toluene (4.0% w/w), and platinum(II) octaethylporphyrinketone (PtOEPK, from Frontier Scientific, Logan, USA) were added to the solution in variable proportions (from 0.025% to 0.4% w/w with respect to PS). Glass plates (49 mm x 49 mm x 1 mm) were cleaned with a sequence of 2 min ultrasonic baths in acetone and isopropanol, rinsed with deionized water and dried with nitrogen flow. PS/PtOEPK films were then fabricated by spin-coating first 200 µl of hexamethyldisilazane (HMDS), and immediately after that 200 µl of PS/PtOEPK-toluene solution, both at 3000 rpm for 60 s under cleanroom conditions. The HMDS pre-treatment was found to increase significantly the adhesion between glass and PS films. Immediately after spin coating the plates were placed on a hot plate (T = 100°C) for 10 minutes, and then left for overnight drying. This coating procedure resulted in films with the average thickness of 480 nm (measured with Bruker Dektak XT contact profilometer), which is in the same range as the reported spin coated PS and PS-PtOEPK film thicknesses in [20, 21]. Before any use, the sensing plates were bathed in DI-water for 48 h at room temperature to ensure the stable film adhesion.

Optical set-up of the sensor
The lenses, filters and LED (LED591E, 590 nm, 2 mW) needed in the set-up shown in Fig. 2a were from Thorlabs, Germany. The parabolic lens was manufactured by Jenoptik, Germany, and made of polystyrene, which caused some additional aberrations at the glass plate - polystyrene lens - interface that are neglected in the analysis. Optical contact between the glass plate and the parabolic lens was assured with immersion oil (n = 1.51).

The oxygen-induced changes in the fluorescence lifetime were measured by a quadrature synchronous detection with a tailored hardware. The excitation LED was driven using 2 kHz square wave current (20 mA peak-to-peak), and the fluorescent emission was detected with a photodiode (S1226-18BQ). The synchronous detector had a bandwidth of 23 Hz and its I/Q outputs were sampled to produce phase angle measurements at a data rate of 10 Hz. The LED excitation signal was used as a phase reference.

Sensor Calibration
Sodium sulfite (Na_2SO_3, from Merck, Germany) was used as chemical deoxygenator (1 g Na_2SO_3 dissolved in 100 mL of deionized water) in some calibration measurements.

Set-up in cell experiments
The set-up used in the experiments with the cardio myocytes is schemed in Fig. 4a. A tailored PDMS 1-well culture chamber with a volume of 1 mL (Fig. 4b, see also [22,23]) is mounted directly on the sensing film (film thickness 480 nm, PtOEPK/PS ratio 0.1%) on the oxygen sensing plate. The bottom of the culture chamber has a round opening (diameter 3.5 mm), operating as a cell area, where the cells can be plated. The culture chamber is closed with a transparent polycarbonate lid, and the

structure is covered with a 3D-printed cover made of UV curable acrylic plastic. This arrangement creates a small volume gas environment around the PDMS structure, which enables one to control the gas content of the culture medium. In addition, the cover is equipped with a glass window so that on-line microscopy is possible from the top. The glass plate containing the PDMS culture well is placed on a commercial transparent ITO heater plate (Okolab 401, glass thickness 0.5 mm) and the pO_2-sensor optics is placed in contact with the heater plate. Optical contacts in both sides of the heater plate are assured with the immersion oil (n = 1.51). For the upright microscopy, a PointGrey camera (FL3-U3-13E4M-C) equipped with a Nikon 10x objective (Ph1 ADL 10x Inf. corrected) is attached to a motorized z-stage. For microscopy illumination purposes, a green LED (532 nm) and 3 x 3 x 1 mm glass diffuser are mounted inside the pO_2 –sensor head, on the optical axis of the system, just underneath the parabolic lens. This arrangement results in some losses in fluorescence collection efficiency, but as the most of the emission power is radiated into the super-critical angles and therefore collected through the outer parts of the parabolic lens, it is not critical. Finally, the heater plate is fixed in a tailored metallic frame mounted in a xyz-stage enabling accurate adjustments. The illumination control, video recording and pO_2 sensor recording is controlled through Matlab-interface.

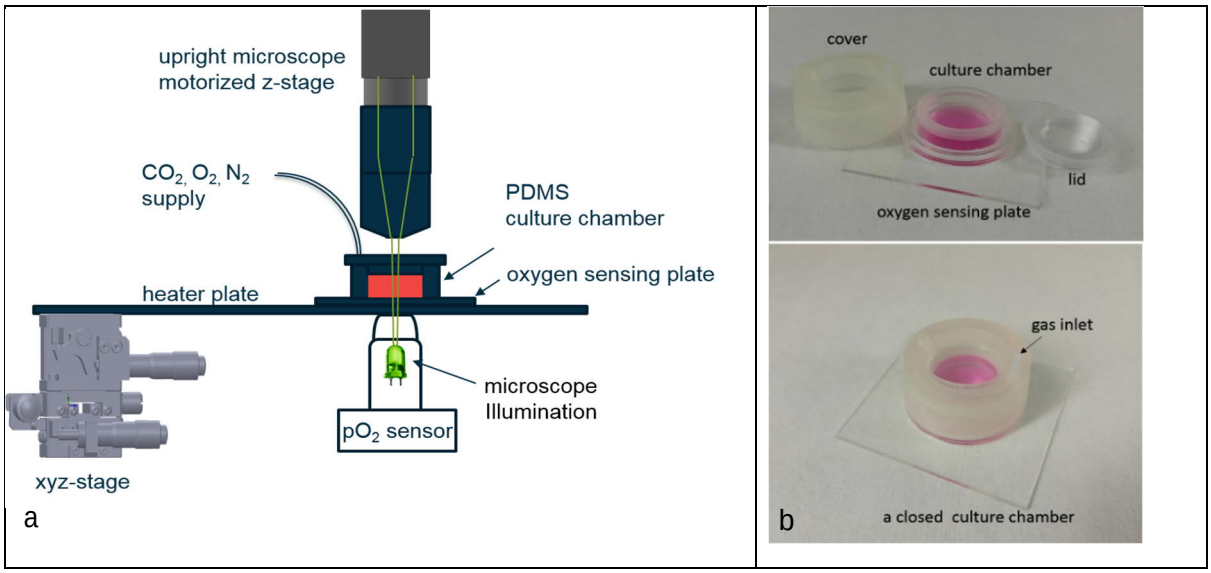

Fig. 4. (a) The scheme of the tailored cell culturing system; (b) the parts of the cell culture chamber.

iPS-cardiomyocyte culture

Cardiomyocytes (CM) were derived from human iPS-cell line UTA.04602.WT as previously described in [24]. For sterilization, the oxygen sensing plates were immersed in 70% ethanol for 2 h and dried under sterilized conditions. PDMS 1-well culture chambers were mounted on the sterilized plates, directly on the PtOEPK/PS films. Beating iPS-CM aggregates were plated on the cell well bottom, which was first hydrophilized with FBS and then coated with 0.1% gelatin type A (Sigma-Aldrich, St Louis, MO, USA). The iPS-CMs were cultured in KO-DMEM-media (Lonza, Basel, Switzerland) with 20% FBS (Lonza), 1% non-essential amino acids (NEAA) (Cambrex, East Rutherford, NJ), 2 mM Glutamax (Invitrogen, Carlsbad, CA), 50 U/ml penicillin/streptomycin (Lonza). For each cell well, 3-4 iPS-CM aggregates were plated. After plating, the iPS-CM aggregates were cultured in an incubator (T = 37°C, 5% CO2, 19% O2, 76% N2) for initial stabilization for 12 h.

4. Results and discussion

4.1 Sensor performance

In order to reveal the presence of any autofluorescence from the glass substrate, the polystyrene film itself or from the LED, the response of the respective samples without PtOEPK were measured. With the maximum available excitation power in our system (100 mA led-current at 2 kHz), no emission

signal (λ > 695 nm) could be seen in the detector. Then the excitation power was adjusted to 20 mA at 2 kHz, and the sensor performance with three PtOEPK/PS films having the same average thickness of d ~ 480 nm but different dye/polymer ratios, was investigated. The sensing surface of the oxygen sensing plate was flushed with a gas containing a variable concentration of O_2 at room temperature and atmospheric pressure, and the sensor phase responses were recorded. Fig. 5 shows the corresponding Stern-Volmer plots, generated according to equation (1), for three different PtOEPK/PS ratios. In Fig. 5a, a separately measured constant phase lag $\phi_c = 16.5°$ between the LED excitation and photodiode amplifier signal, has been subtracted from all phase values before the division in equation (1). The figure shows very similar linear Stern-Volmer characteristics for the two highest PtOEPK/PS ratios, but the film with the lowest PtOEPK/PS ratio has a clearly less linear response. However, our phase detection hardware is not totally immune against to the change in overall signal level, which takes place when the film with the lowest concentration is used. This is demonstrated in Fig. 5b, where we have used a separate best-fit value of ϕ_c for each film. This procedure improves the performance in all cases, and almost perfectly linearizes the Stern-Volmer characteristics also for the film with the lowest PtOEPK/PS ratio, where now only a minor deviation at high oxygen concentrations can be seen. The sensor characteristics, as well as the used best-fit values of ϕ_c, are summarized in Table 1. The presented sensitivity values are calculated by solving (1) for ϕ and taking the derivative with respect to pO_2.

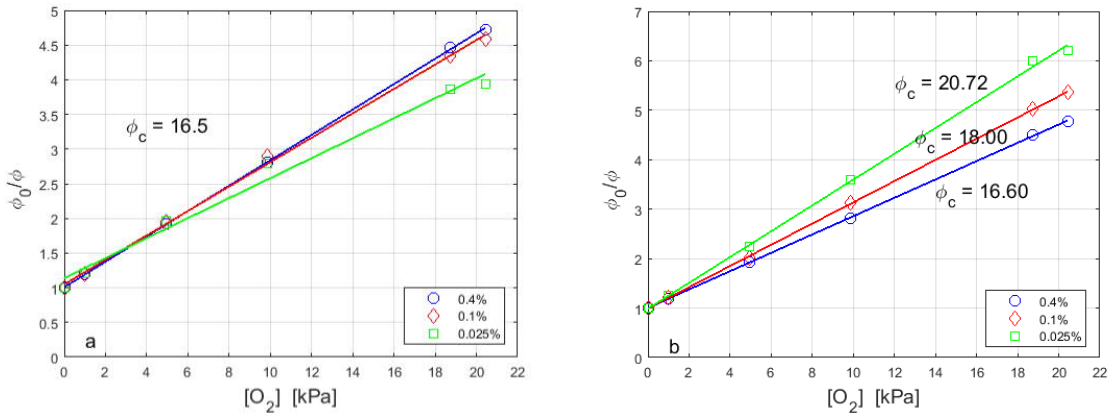

Fig. 5. Stern-Volmer plots with three different PtOEPK/polystyrene ratios. (a) with the same phase constant; (b) with best-fit phase-constants.

The noise values shown in the table are measured at pO_2 = 5 kPa. It is well-known that the noise-level of an oxygen sensor based on oxygen dependent fluorescence quenching is pO_2 dependent: the lower the pO_2 the less quenching takes place, which results in higher signal amplitudes and the lower noise levels also in phase detection. Overall, the noise levels of our device are clearly comparable with commercial devices [18, 19], but accurate comparison of signal-to-noise ratio is difficult since the bandwidth information of the commercial devices is often unclear.

Table 1. Oxygen sensor characteristics with different PtOEPK/polystyrene -ratios.

PtOEPK/ PS [%]	ϕ_c [°]	K_{SV} [kPa^{-1}]	Sensitivity [°/kPa] (at pO_2 = 5.0 kPa)	Phase noise [° rms] (at pO_2 = 5.0 kPa at 10 Hz data rate)	pO_2 noise [kPa rms] (at pO_2 = 5.0 kPa at 10 Hz data rate)
0.400	16.60	0.185	-1.97	0.0076	0.0039
0.100	18.00	0.215	-1.87	0.019	0.010
0.025	20.72	0.261	-1.66	0.050	0.030

In order to study in more details the emission characteristics of the used PtOEPK/PS films, and the performance of the proposed collection optics, we replaced the photodiode in the optics scheme in

Fig. 3a with a monochrome camera (Point Grey Grashopper3 GS3-U3-91S6M). The distance between the parabolic lens bottom and the collection lens was adjusted to 145 mm, so that the complete parabolic bottom surface could be imagined. All structures between the parabolic lens and the collection lens were removed, and a focused excitation beam (beam waist ~ 1.1 mm) was directed to the PS/PtOEPK film (d ~ 480 nm) through an excitation filter (FGL38) from above in a 45° angle. To make the results comparable with the simulations, the sensing film was covered with a 1 mm layer of water. Fig. 6a shows an image of the measured fluorescence emission. In the central area, we can see the contribution of the direct radiation that could be detected with non-contact optics. The large ring-like structure, in turn, is formed by the super critical angle emission that is being internally reflected by the parabolic part of the lens between the flat upper and lower surfaces of the lens (marked as red dashed lines in the picture). The picture demonstrates how the peak irradiance lies within the range of supercritical angles, and that the total signal collected over the supercritical range of angles exceeds many times the signal that can be collected in the middle area. In more details, the data shown in Fig. 6a is used first for the calculation of a co-centric mean irradiance distribution (in 0.0985 mm steps) as a function of the distance from the centre of the excitation beam. Due to the geometry, within the range of angles that are reflected by the parabolic edge, every co-centric ring of irradiance corresponds to a single emission angle from the polystyrene film to the glass substrate. This calculation results in the angular emission distribution shown as blue line in Fig. 6b. The angular radiation distribution of the direct radiation in the middle area is shown as a red line, where the instant drop of the level is exaggerated by the large distance of the collecting lens. Comparing the measured super critical angle distribution with the simulated distributions in Fig. 3b, one can notice how closely the shape of the measured distribution resembles the shape of the simulated ones for 400 nm and 500 nm films. In the measurements, however, the maximum value is shifted about five degrees to the direction of smaller angles, which can be explained by the refractive index mismatch between the glass substrate and the polystyrene parabolic lens. Due to this mismatch, all super critical emission angles at the glass substrate/polystyrene lens interface are refracted more towards the optical axis, which results in a shift towards larger distances from the axis and, therefore, in smaller calculated emission angles in Fig. 6b. Another way to interpret this shift is to recall that the simulations with d = 400 and d= 500 m resulted in peak irradiance at the critical angle between water and the substrate. As the glass thickness is 1 mm and the polystyrene parabolic lens thickness is 12.1 mm, the substrate can be seen as mainly polystyrene, so the peak irradiance should be found close to the critical angle between water and polystyrene θ_c = 56.8°, which is good agreement with the measurements. It is also noteworthy that the measured ratio (~ 2) of the peak irradiance to the irradiance in the middle is in agreement with the simulations.

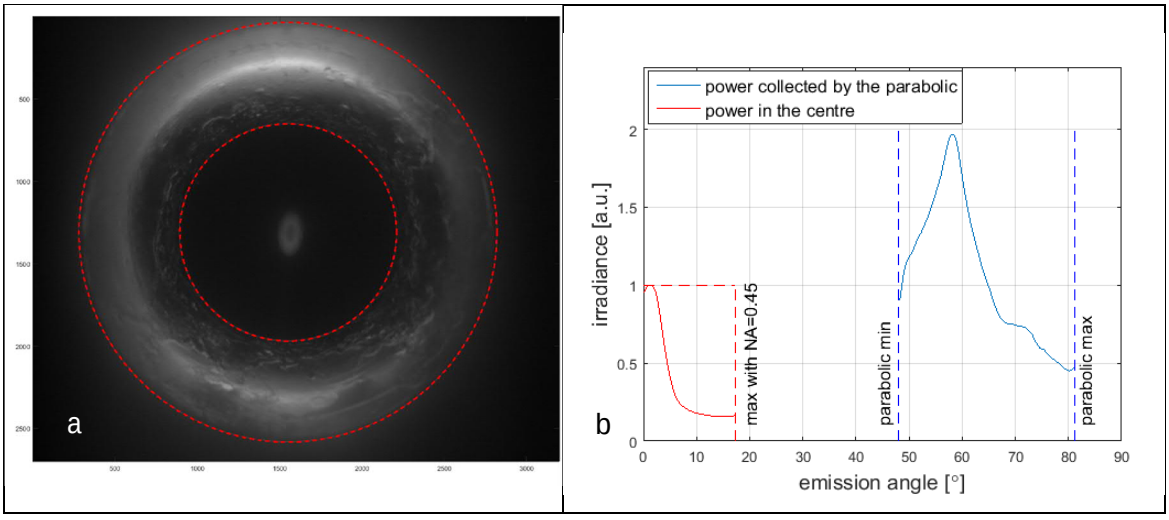

Fig. 6. (a) A picture of the fluorescence emission distribution under the parabolic lens. The locations of the upper (in contact with the sensing plate) and lower surfaces of the lens are marked as red dashed lines; (b) The calculated co-centric mean irradiance as a function of the emission angle from the polystyrene film into the glass.

Finally, we can estimate (overestimate) that the absolute maximum power detectable with NA = 0.45 non-contact optics under a glass substrate is the power measured in the middle over the whole range of detectable emission angles (from polystyrene into glass) up to 17.2°, where the upper limit comes from the geometry and refractive indices of glass and air (marked with the dashed red line). Here, this estimation results in a power ratio of ~ 2.0 between the detected supercritical angle power and the estimated absolute maximum power detectable with NA = 0.45. Taking into account that for the d = 500 nm films, our parabolic lens can collect 83% of the trapped light, also this estimated power ratio is in approximate agreement with the calculations in Fig. 2b.

Although these results are clearly supportive to the simulation results and the suggested optical read-out, it should be emphasized that a more detailed analysis and more rigorous experimental verification of the emission distribution would require a more suitable set-up, such as used with LED development in [12]. However, the construction of such a different set-up is out of the scope of this paper. Instead, we proceed to show some preliminary results when the device is applied to the pO_2 monitoring of cardiomyocyte cultures, which highlights some additional advantages of the system.

4.2. Cell experiments

While in the characterization measurements the substrate thickness was 1.0 mm, in cell experiment set-up the heating plate contributes with additional 0.5 mm glass thickness (Fig. 4). This results in diminished performance as the used parabolic lens is tuned for 1.0 mm substrates. We mitigated this to some extent by grinding additional 0.5 mm away from the upper surface of the lens.

Calibration at T = 37°C

Fig. 7 shows the phase response of the oxygen sensor, in the cell experiment set-up, at different temperatures in water, and in water deoxygeneated with Na_2SO_3. According to the measurements in water (Fig. 7a), the phase difference decreases 1.20° as the temperature increases from T = 25°C to T = 37°C. At the used 2 kHz modulation frequency, this corresponds to decrease of 1.67 µs in the fluorescence lifetime, or 0.54% per 1°C if we assume τ = 26 µs for the PtOEPK fluorescence lifetime in PS in air-saturated water [27].The shortening of the lifetime is induced by the increased thermal quenching and faster oxygen diffusion in PS [17]. In addition, the temperature dependence of the read-out electronics contributes to the change, but as the electronics closure is separated from the heater plate, the contribution is negligible.

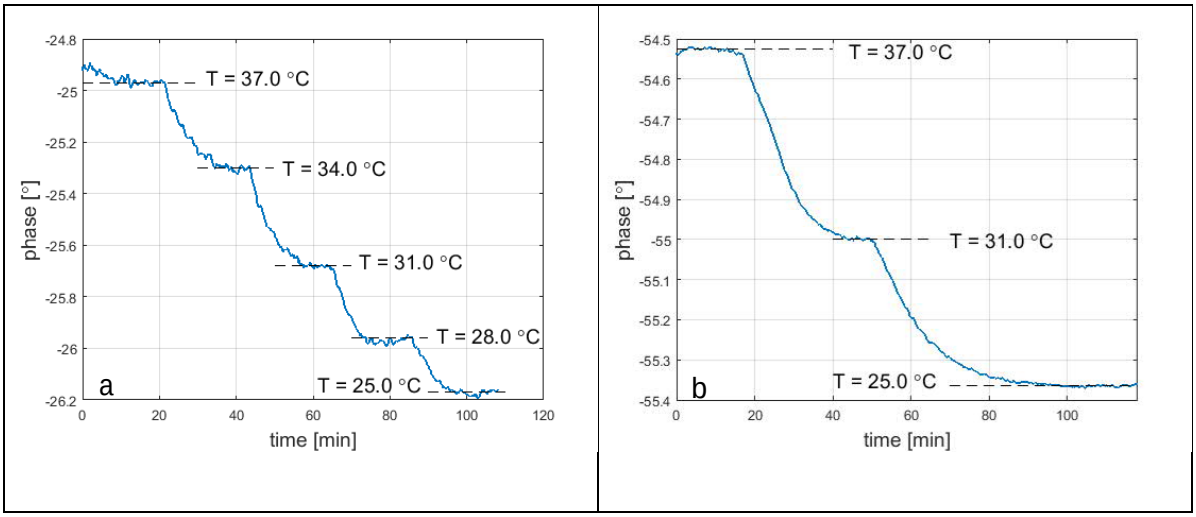

Fig 7. The phase response of the pO_2 sensor at different temperatures in water (a) and in de-oxygenated water (b).

In deoxygenated water (Fig. 7b) the corresponding change is 1.17 µs or 0.16% per 1°C, where the unquenched lifetime τ_0 = 60 µs have been used as reference [27]. Here, as the oxygen diffusion does not have an impact in deoxygenated conditions, the decrease in the lifetime is probably mainly due thermal quenching. The value of 0.16% per 1°C is in agreement with previous findings for Pt(II) metalloporphyrins [5].

Fig. 8 shows the Stern-Volmer plot at T = 37°C, where two additional points (at 5.0 and 10.0 kPa) have been generated by directing a constant flow of pre-heated gas mixture of known oxygen content to the preheated oxygen sensing plate. For comparison, the Stern-Volmer plot for the same plate type (0.1% PtOEPK/PS) at T = 25°C is also shown. The phase lag constant is held as ϕ_c = 18.0 in both plots, as it corresponds to the unchanging basic phase lag value between the LED excitation and photodiode signal. The change in the Stern-Volmer plots between T = 25°C and T = 37°C is relatively small, and the increase in Stern-Volmer constant with increasing temperature is in agreement with the arguments above and [19].

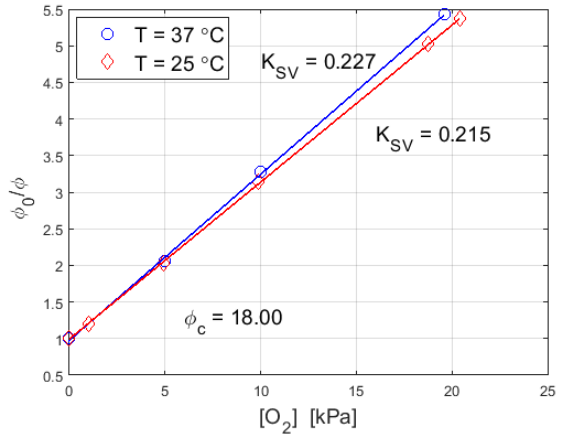

Fig. 8. The Stern-Volmer plots at T = 25°C and T = 37°C.

Monitoring cardiomyocytes

After the iPS-CMs were plated in the PDMS culture chamber, mounted on an oxygen sensing plate as described earlier, the iPS-CMs were cultured first in an incubator (T = 37°C, 5% CO2, 19% O2, 76% N2) for 12 h. Then the culture chamber was closed with the lid and the cover, and the plate was placed on the heater plate, calibrated for T = 37°C. The baseline oxygen conditions were established by flushing the gas environment around the culture chamber with a constant flow (5 $mLmin^{-1}$) of a gas mixture containing 19% of O_2, 5% CO_2, and 76% of N_2. Oxygen recordings were carried out every 10 minutes and a one-minute long video at 45 frames per second was recorded once an hour. These videos were later analysed according to methods described in [28].

Fig. 9a shows the induced oxygen tension during 40 h of such a test. After 4 h of baseline recording, the system was set towards hypoxic conditions by switching into a gas mixture containing 1% of O_2, 5% of CO_2 and 94% of N_2. In about 3 h, the system had reached a stage close to the oxygen condition of pO_2 = 2 kPa. This is slightly more than what the set point of 1% should yield. This is probably due to some leakage in the sealing of the system. The essentially unchanged post-calibration after the completed tests (data not shown) supported this hypothesis. The first hypoxic period lasted 12 h, and then the system was returned to the baseline conditions for a short time until a second hypoxic period took place.

In Fig. 9b, the average beating frequencies, analysed from the videos as in [28], are plotted together with the respective pO_2 sensor output during the first hypoxic period. According to this small data set,

it remains questionable whether there exists a direct correlation between the pO_2 tension and the beating frequency. A slight indication of a correlation can be seen, as well as some interesting anomalies. Especially at 7.6 h, the beating frequency has a great deviation, and interestingly this happens at the same time when there is also an anomaly in the pO_2 sensor output. In principle, a rise in the temperature could cause both deviations, but a closer analysis in the pO_2 sensor data reveals that this would indicate approximately a 6°C rise in the temperature for about 1 h, which would have been lethal for the cells. However, as the temperature sensor recording failed during the first 24 h, the possibility of a period of elevated temperatures cannot be absolutely excluded.

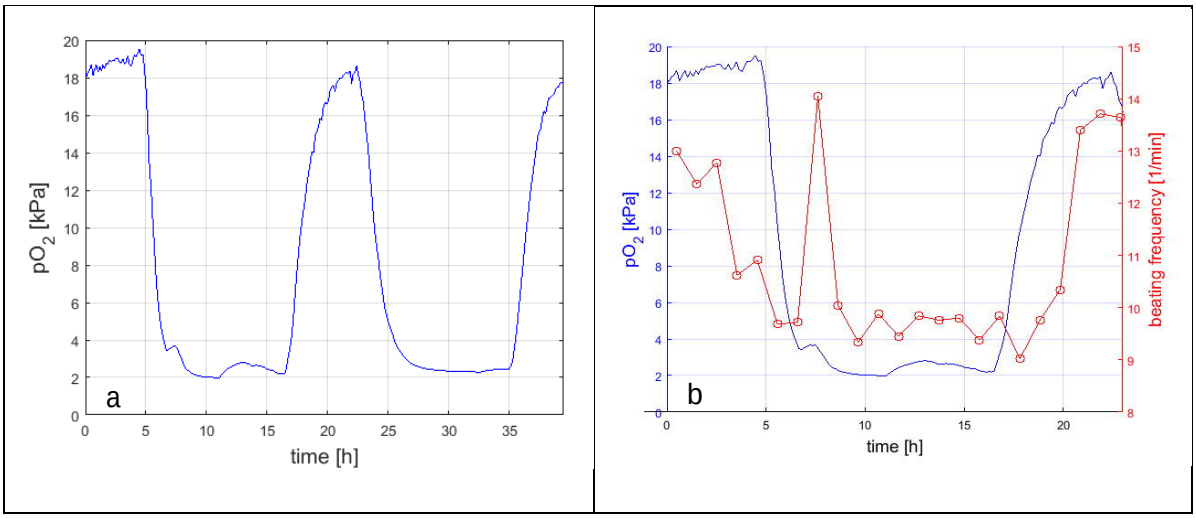

Fig. 9. Applying the oxygen sensor into the pO_2 control of beating cardiomyocyte cultures. (a) The pO_2 output of the sensor; (b) The pO_2 output together with the beating frequency of the followed cluster during the first hypoxic period.

4.3. Discussion

The presented results with cardiac cells are only very preliminary. They serve here as exemplary experiments highlighting the performance and the features of the developed oxygen sensor. More tests, repetitions, and further equipment development and tuning are needed for achieving rigorous results from the point of view of cell research. However, in our tests, the cardiac cell aggregates from the used cell line could endure the sensing surface with PtOEPK/PS ratio of 0.1% more than five days (three repetitions in total). This means that for the many coming tests with these cells, it is probable that no additional biocompatible shielding layer is needed.

As such, the reported device is only a single-spot pO2 –sensor, but it could be turned into an imaging or a multi-spot sensor by integrating a scanning mechanism in the device. We have found that with the current geometry, a glass plate with the spin-coated PtOEPK-PS film can be moved in the xy-plane over 1 mm without any change in the measured phase difference. For the scanning purposes a digital mirror device could be a good option [29]. However, even in a single-spot sensing, the presented detection scheme can have a justified use in applications such as the oxygen control of cell cultures, where the biocompatibility issues are very important and the dye concentrations and the excitation power radiated into the cell chamber must be minimized. In addition, the geometry of the detection scheme gives freedom to integrate other instruments, such as microscope illumination devices, temperature sensors, microelectrode arrays (MEAs) the centre of the cell area.

5. Conclusions

Based on electromagnetic simulations, and on an optical detection scheme utilising an in-contact parabolic lens, an efficient way for collecting the fluorescence stemming from a thin dye-polymer

film deposited on a glass-water interface has been demonstrated. It has been shown how the use of parabolic lens also facilitates a confocal total internal reflection excitation from the substrate side. This makes the excitation effective, and importantly, greatly reduces the amount of excitation power radiated to the cell culture chamber. As both the excitation and the main part of read-out are strictly focused on sensing film, the arrangement is insensitive to autofluorescence and other background signals stemming from the sample side. This is feature is further emphasized if the direct radiation in the centre of the sensing are is excluded from the fluorescence detection. The experimental results with a phase fluorimetric oxygen sensor, taking advantage of the developed optical read-out, and 480 nm PtOEPK/PS films having 0.025% dye/polymer ratio, showed sensor characteristics comparable to commercial devices. The set-up can be especially useful when the biocompatibility issues are important, and the dye concentration and the excitation power must be minimized. In addition, it has been shown how the optical arrangement leaves space for other instrumentation such us microscopy illumination in the centre of the sensing area and how the arrangement can be integrated together with an ITO heating plate in an *in vitro* cell monitoring system. Finally, it has been demonstrated how the developed sensor system can be applied to an on-line cell culture monitoring, such as on-line video analysis of beating cardiomyocytes under pO_2 stress.

Acknowledgement

The Financial support by TEKES, the Finnish Funding Agency for Technology and Innovation, is gratefully acknowledged.

References

[1] D. F. Wilson, Quantifying the role of oxygen pressure in tissue function. Am. J. Physiol.: Heart Circ. Physiol. 294 (2008), H11-H113.
[2] D. Papkovsky and R. Dmitriev, Biological detection by optical oxygen sensing. Chem. Soc. Rev. 42 (2013), 8700-8732.
[3] C. Wu, T. Yasukawa, H. Shiku, T. Matsue, Fabrication of miniature Clark oxygen sensor integrated with microstructure. Sens. Actuators, B 110 (2005), 324-349.
[4] S. Grist, L. Chrostowski, K. Cheung, Optical Oxygen Sensors for Applications in Microfluidic Cell Culture. Sensors 10 (2010), 9286-9316.
[5] M. Quaranta, S. Borisov, I. Klimant, Indicators for optical oxygen sensors. Bioanal Rev 4 (2012), 115-157.
[6] X-D Wang and O. Wolfbeis, Optical methods for sensing and imaging oxygen: materials, spectroscopies and applications. Chem. Soc. Rev. 43 (2014), 3666-3761.
[7] S. O'Driscoll, McEvoy, C. McDonagh, B. MacCraith, Enhanced Fluorescence-Based Optical Sensor Performance Using a Simple Optical Collection Strategy. IEEE Photonics Technology Letters, 6(24), 2012.
[8] R. Blue, N. Kent, L. Polerecky, H. McEvoy, D. Gray and B.D. MacCraith, Platform for enhanced detection efficiency in luminescence-based sensors. Electrinics Letters, 12(41), 2005.
[9] L. Polerecky´, J. Hamrle, and B.D. MacCraith, Theory of the radiation of dipoles placed within a multilayer system. Appl. Opt. 38 (2000), 3968-77.
[10] P. Ceroni, A. Lebedev, E. Marchi, M. Yan, T. Esipova, G. Bergamini, D. Wilson, T. Busch, S. Vinogradov, Evaluation of dentritic porphyrin-based phosphorescent oxygen probes: an *in vitro* study. Photochem Photobiol Sci. 10(6) (2011), 1056-1065.
[11] W. Lukosz and R. E. Kunz, Light emission by magnetic and electric dipoles close to a planar interface. I. Total radiated power, J. Opt. Soc. Am. 67 (1977) 1607-15.
[12] J. Frischeisen, D. Yokoyama, C. Adachi, W. Brütting, Determination of molecular dipole orientation in doped fluorescent organic thin films by photoluminescence measurements. Appl. Phys. Lett. 96 (2010), 073302.
[13] S. Nowy, B. C. Krummacher, J. Frischeisen, N. A. Reinke, W. Brütting, Light extraction and optical loss mechanisms in organic light-emitting diodes: Influence of the emitter quantum efficiency. J. Appl. Phys. 104 (2008), 123109.
[14] J. Enderlein, T. Ruckstuhl, S. Seeger, Highly efficient optical detection of surface-generated fluorescence. Appl. Opt. 38 (1999), 724-732.
[15] D. Kurzbuch, J. Bakker, J. Melin, C. Jönsson, T. Ruckstuhl, B.D. MacCraith, A biochip reader using super critical angle fluorescence. Sensors and Actuators B 137 (2009) 1–6.
[16] H. Välimäki and K. Tappura, A novel platform for highly surface-sensitive fluorescence measurements applying simultaneous total internal reflection excitation and super critical angle detection. Chem. Phys. Lett. 473 (2009), 358-362.
[17] K. Koren, S. Borisov, I. Klimant, Stable optical oxygen sensing materials based on click-coupling of fluorinated platinum(II) and palladium(II) porphyrins – A convenient way to eliminate dye migration and leaching. Sens. Actuators, B 169 (2012), 173-81.
[18] E. Hecht, Optics, 4th ed., Addison Wesley, San Francisco, 2002.
[19] J. Lakowicz, Principles of Fluorescence Spectroscopy, 3rd ed., Springer US, New York, 2006.

[20] V. Nock, R. Blaikie, T. David, Patterning, integration and characterisation of polymer optical oxygen sensors for microfluidic devices. Lab Chip 8 (2008), 1300-1307.
[21] D. Hall, P. Underhill, J. Torkelson, Spin Coating of Thin and Ultrathin Polymer Films, POLYM ENG SCI 38(12) (1998), 2039-2045.
[22] J. Kreutzer, K. Rantanen, H. Välimäki, J. Lekkala, P. Jaakkola, P. Kallio, Mini-incubator For Prolonged Cell Culture And Hypoxia Studies Outside An Incubator. *Front. Neurosci. Conference Abstract: MEA Meeting 2016 | 10th International Meeting on Substrate-Integrated Electrode Arrays.* doi: 10.3389/conf.fnins.2016.93.00043
[23] J. Kreutzer, L. Ylä-Outinen, A. Mäki, M. Ristola, S. Narkilahti, P. Kallio, Cell culture chamber with gas supply for prolonged recording of human neuronal cells on microelectrode array. Journal of Neuroscience Methods 280 (2017), 27-35.
[24] A. Lahti, V. Kujala, H. Chapman, A. Koivisto, M. Pekkanen-Mattila, E. Kerkelä, J. Hyttinen, K. Kontula, H. Swan, B. Conklin, S. Yamanaka, O. Silvennoinen, K. Aalto-Setälä, Model for long QT syndrome type 2 using human iPS cells demonstrates arrhythmogenic characteristics in cell culture. Dis Model Mech. 5(2) 2012, 220-30.
[25] https://www.presens.de/fileadmin/user_upload/brochures/Web_Presens_O2_Broschuere_08-16.pdf, 14.1.2017
[26] https://www.wpiinc.com/clientuploads/pdf/DS/OxyMicro.pdf, 14.1.2017
[27] C. O'Donovan, J. Hynes, D. Yashunski, D. Papkovsky, Phosphorescent oxygen-sensitive materials for biological applications. J. Mater. Chem. 15 (2005), 2946–2951.
[28] A. Ahola, A. Kiviaho, K. Larsson, M. Honkanen, K. Aalto-Setälä, J. Hyttinen, Video image-based analysis of single human induced pluripotent stem cell derived cardiomyocyte beating dynamics using digital image correlation. Biomed Eng Online, 13:39 (2014), 1–18.
[29] S. Chao, M. Holl, S. McQuaide, T. Ren, S. Gales, D. Meldrum, Phosphorescence lifetime based oxygen microsensing using a digital micromirror device. Optics Express 17(15) (2007), 10681-10689.